ARTICLES

Tensor analyzing powers for ^{2}H$(d,p)^3$H and ^{2}H$(d,n)^3$He at deuteron energies of 25, 40, 60, and 80 keV

K. A. Fletcher,* Z. Ayer, T. C. Black, R. K. Das,† H. J. Karwowski, and E. J. Ludwig
Department of Physics and Astronomy, University of North Carolina at Chapel Hill, Chapel Hill, North Carolina 27599 and Triangle Universities Nuclear Laboratory, Duke University, Durham, North Carolina 27708

G. M. Hale
Theoretical Division, Los Alamos National Laboratory, Los Alamos, New Mexico 87545
(Received 31 January 1994)

Angular distributions of the tensor analyzing powers A_{zz} and $A_{xx} - A_{yy}$ for the reactions ^{2}H$(d,p)^3$H and ^{2}H$(d,n)^3$He are presented at deuteron energies of 25, 40, 60, and 80 keV. The analyzing powers for the two reaction channels are quite similar at these energies. The data have been included in an R-matrix analysis of the four nucleon system. According to this analysis, transitions from entrance-channel quintet-S states are important in these reactions, so that the use of polarized fuels would not result in a neutron-lean fusion reaction.

PACS number(s): 21.45.+v, 24.70.+s, 25.10.+s, 25.45.−z

INTRODUCTION

The ^{2}H$(d,p)^3$H and ^{2}H$(d,n)^3$He reactions have been studied since the early days of nuclear physics [1]. These reactions merit continued study for both fundamental and practical reasons. From a fundamental point of view, the ^{2}H+^{2}H reactions possess many interesting properties, such as identical bosons in the entrance channel, charge symmetry in the exit channel, and contributions from P and D waves even at very low energies. In contrast to the three-nucleon system, in the $A = 4$ system excited states exist which can influence the scattering processes. These reactions play an important role for primordial nucleosynthesis and in fusion energy research. The ^{2}H+^{2}H reactions have been discussed in recent reviews of the four-nucleon system [2,3].

The reactions are governed by very complex reaction mechanisms, even at very low energies. Brown and Jarmie [4] measured cross sections with 2% accuracy from 20 to 117 keV using a windowless gas target. Kraus *et al.* [5] measured angular distributions using a gas jet target over an energy range of 15–330 keV and excitation functions from about 6 to 325 keV. Despite small disagreements between the two data sets, both groups concluded that there are no sharp resonances at these energies, that there is larger angular asymmetry for ^{2}H$(d,n)^3$He than for ^{2}H$(d,p)^3$H, and that D waves are important at energies above about 60 keV. These data indicate that the ^{2}H$(d,p)^3$H and ^{2}H$(d,n)^3$He reactions are governed by transitions from S, P, and D waves in the entrance channel, even at laboratory energies below 80 keV. The presence of higher-order partial waves greatly increases the complexity of the reaction mechanism. Such unexpectedly high orbital angular momenta in the entrance channel are probably due to the large interaction radius for the participating deuterons. In a transition matrix element analysis by Ad'yasevich, Antonenko, and Fomenko [6,7], which has been extended by Lemaître and Schieck [8], 16 complex matrix elements (ME's) were included for each reaction.

Several groups have reported analyzing power measurements of the ^{2}H$(d,p)^3$H and ^{2}H$(d,n)^3$He reactions in the last few years. Pfaff *et al.* [9,10] have measured all four analyzing powers (A_y, A_{zz}, A_{xz}, and $A_{xx} - A_{yy}$) at laboratory energies from 80 to 460 keV, for both reactions, although to date these data have not been published. These data were used in [8] to produce a transition matrix element fit at energies below 500 keV. In this analysis, the energy dependence of the matrix elements was assumed to result entirely from the Coulomb penetrability in the entrance channel. The same group has reported on a new transition matrix element fit which includes their own measurements of four independent analyzing powers for both reactions at $E_{\rm lab} = 28$ keV [11]. Analyzing power measurements have also been reported for the ^{2}H$(d,p)^3$H reaction only at deuteron energies of 30, 50, 70, and 90 keV [12].

*Present address: Department of Physics and Astronomy, State University of New York at Geneseo, Geneseo, NY 14454
†Present address: Radiation Oncology Center, Mallinckrodt Institute of Radiology, Washington University School of Medicine, St. Louis, MO 63110.

0556-2813/94/49(5)/2305(6)/$06.00

Information obtained for these reactions contributes to a global analysis of the ^{4}He system. Such an analysis for the four-nucleon system using the R-matrix formalism is underway at Los Alamos National Laboratory (LANL) [13]. This R-matrix parametrization of existing data has been used to determine the broad, overlapping energy levels in ^{4}He [3]. The R-matrix results agree well with those obtained from a resonating group model analysis [14].

It is interesting to note that the data of [11] at 28 keV show slight differences between the two reactions for the polarization observable $(A_{xx} - A_{yy})$ and, for this observable, disagree with R-matrix predictions. The 30-keV measurements from [12], however, are consistent with the R-matrix predictions for $^2\mathrm{H}(d,p)^3\mathrm{H}$.

Data on these reactions are of technical interest as well. Kulsrud *et al.* [15] suggested that polarizing the nuclei in a $^3\mathrm{He}(d,p)^4\mathrm{He}$ fusion plasma reactor could suppress the less energetic $^2\mathrm{H}(d,p)^3\mathrm{H}$ and $^2\mathrm{H}(d,n)^3\mathrm{He}$ reactions, resulting in a more efficient neutron-lean reactor. To significantly suppress the $^2\mathrm{H}+^2\mathrm{H}$ reaction rates in this manner, transitions from the entrance quintet S state must be small. Arguments based on the Pauli principle [1,16] have been used to predict that two deuterons with identical quantum numbers would not interact, but as noted in [16], such arguments are weak because of the large interaction region for the two deuterons. The measurement which would answer this question directly, involving a polarized beam and polarized target, has not been made at low energies. However, analyzing power data can be used to determine the magnitudes of the quintet S-state transitions indirectly.

In this work, we present our simultaneous measurements of the $^2\mathrm{H}(d,p)^3\mathrm{H}$ and $^2\mathrm{H}(d,n)^3\mathrm{He}$ analyzing tensors A_{zz} and $A_{xx} - A_{yy}$ at deuteron energies of 25, 40, 60, and 80 keV. The data have been included in the LANL R-matrix analysis.

EXPERIMENT

The data were obtained at the Low Energy Beam Facility (LEBF) at Triangle Universities Nuclear Laboratory (TUNL). Positively charged, polarized deuteron beams were produced by the TUNL atomic beam polarized ion source [17–19]. Beam currents were typically limited to 1–2 μA to minimize target deterioration. The data collection scheme required three beam polarization states: unpolarized, positive tensor polarized, and negative tensor polarized. For the two polarized states used in our work, the maximum theoretical values for the tensor polarizations (P_{zz}) were +1 and −1 for the 40-, 60-, and 80-keV data. Improved transition units on the polarized ion source enabled use of states with maximum theoretical values of P_{zz} of +1 and −2 for our final run at 25 keV. The polarized ion source provided deuteron beams with polarizations which were about 80% of the theoretical maximum for a given state. The beam tensor polarizations were monitored continuously throughout the data collection, as described below.

Thin-film deuterated titanium targets were used for the 40-, 60-, and 80-keV measurements. These were produced by depositing a titanium film (< 20 μg/cm^2) onto 10-μg/cm^2 carbon film substrates mounted onto target rings. The films were heated in an evacuated bell jar to about 400 °C, and deuterium gas was admitted into the bell jar to a pressure of 30 mTorr. The films were permitted to cool and were removed. The deuterium content of targets used for data collection was typically 5×10^{16} atoms/cm^2. The target thicknesses were measured by elastic scattering of deuterons at 6 MeV for selected targets from each batch. For an 80-keV deuterium beam, the typical energy loss was 10 keV, as determined from stopping power data [20].

The small cross section for the 25-keV measurement was compensated by the availabilty of deuterated parapolyphenyl (C_6D_4) thin-film targets with higher deuterium content ($\sim 8 \times 10^{17}$ atoms/cm^2). Deuterated parapolyphenyl powder, produced via a method discussed in [21], was obtained from Y. Tagishi at the University of Tsukuba, Japan. The powder was evaporated onto carbon films. Similar targets were used in [9].

The 30.5-cm-diam, 15.2-cm-tall LEBF scattering chamber was equipped with a slit-control system mounted at the chamber entrance. The current on these vertical and horizontal slits was used to drive a feedback system to control upstream steerers and to maintain a stable beam position on target. Partially depleted, surface-barrier silicon detectors of 100 or 300 μm thickness were used to detect the protons, tritons, and ^{3}He from the reactions. The detectors were placed symmetrically on the left and right sides of the chamber, with three or four detectors on each side. It was essential to place carbon films thick enough to stop the elastically scattered deuterons (about 100–200 μg/cm^2 for our energies) on the collimator slits in front of the detectors. Detector solid angles for the 25-keV measurements were 12.3 msr, corresponding to a total acceptance angle of 7.2 °. For the 40-, 60-, and 80-keV measurements, the solid angles were 4.9 msr ($\Delta\theta = 3.3$ °). The three charged-particle groups were clearly separated in the spectra, as shown in Fig.1, so that the data for both reactions were obtained under the same experimental conditions. The $^2\mathrm{H}(d,p)^3\mathrm{H}$ data were obtained from both the proton and triton peaks, and the $^2\mathrm{H}(d,n)^3\mathrm{He}$ data were obtained from the ^{3}He peaks. Results from the ^{3}H and ^{3}He recoils were converted to the center-of-mass angles for the projectiles.

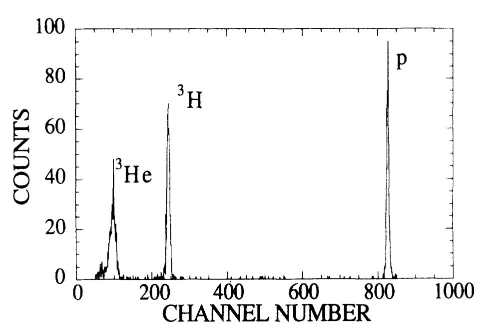

FIG. 1. Energy spectrum for 25-keV deuterons on a deuterated parapolyphenyl target at a laboratory angle of 115 °.

The polarimeter, described in [22], was mounted at the exit of the chamber. For these experiments the same target was used for the beam polarization and analyzing power measurements. This polarimeter consisted of four solid-state detectors placed up, down, left, and right at a laboratory angle of 10 ° to detect reaction products from $^2H(d,p)^3H$. It was calibrated using the A_{zz} measurements of [12], as described in [22]. The polar and azimuthal angles of the spin axis (β and ϕ in the notation of [23]) were established by the Wein filter placed after the ion source. The beam polarization was continuously monitored during the data collection.

Although absolute beam current integration is not necessary for analyzing power measurements, relative beam current integration for the different spin states is quite important. The chamber and polarimeter were isolated from the ground, and all collected charge from the chamber, polarimeter, and target rod was summed at the integrator. The target rod, which was insulated from the chamber, was positively biased to prevent the escape of electrons created in the target. The currents on the target rod and chamber could be separated for diagnostic purposes.

Early tests indicated considerable depletion of the deuterium content of the targets under beam bombardment. If the effective target thickness varies during measurements for each of the three spin states, spurious asymmetries can result; therefore, rapid state switching was employed to reduce the effects of target depletion. The states were switched through a sequence to eliminate first-order effects of target depletion. For the measurements at 40, 60, and 80 keV, the spin states were changed at 1-min intervals, which was deemed adequate based on the target depletion tests. Later improvements to the polarized ion source allowed faster state changing, and for the 25-keV measurement states were changed every few hundred milliseconds.

ANALYSIS

Our data have been included in the data set of the LANL multichannel R-matrix parametrization of the four-nucleon system. The R-matrix approach was introduced in [24], modified in [25], and reviewed in [26]. The LANL R-matrix approach is described in [27,28,13]. Only a brief summary will be given here. The R-matrix elements are given by

$$R_{c'c} = \sum_{\lambda} \frac{\gamma^T_{\lambda c'} \gamma^T_{\lambda c}}{E_\lambda - E}. \quad (1)$$

The R-matrix parameters, the reduced-width amplitudes $\gamma^T_{\lambda c}$, and energies E_λ for the reaction channel c and energy level λ are varied to obtain simultaneously the best fit to all available data for two-body reaction channels below about 20 MeV incident energy. The data set includes total and differential cross sections, vector and tensor analyzing powers, and polarization-transfer coefficients. Parameters which yield the best fit to existing data are determined and can be used to predict other unmeasured observables.

The reduced-width amplitudes have definite isospin T, and for the four-nucleon system T is restricted to 0 or 1. To reduce the number of parameters to be fitted for the channels in the ^{4}He system, the $T = 1$ parameters were deduced from the analysis of the ^{4}Li system, as described in [13]. In the "charge-independent" LANL analysis, R-matrix parameters were first determined from the data for p-^{3}He. These results were then tested by applying a Coulomb energy shift to the energy levels E_λ and calculating the total cross section and S-wave scattering lengths for n-^{3}H. These energy-shifted parameters were found to satisfactorily reproduce the data for n-^{3}H. The p-^{3}He parameters, with appropriate energy shifts, were then used to determine the $T = 1$ parameters for the p-^{3}H and n-^{3}He channels in the ^{4}He system. The $T = 0$ parameters for the channels ^{2}H-^{2}H, p-^{3}H, and n-^{3}He were varied to fit the data. The data are well represented by the set of partial waves $L \leq 3$.

A CRAY X-MP computer was used for the analysis, and the minimization was permitted to continue until the objective function did not change appreciably with subsequent iterations. The present data were the first $^2H(d,p)^3H$ and $^2H(d,n)^3He$ tensor analyzing powers below 150 keV included in the LANL analysis.

RESULTS

Angular distributions of the tensor analyzing powers A_{zz} and $A_{xx} - A_{yy}$ for the $^2H(d,p)^3H$ and $^2H(d,n)^3He$ reactions are shown in Figs. 2 and 3. In general, there are twice as many data points for the $^2H(d,p)^3H$ plots because both reaction products were detected for this reaction. The energy loss in the target was used to determine a target-averaged reaction energy for the observables. These energies are reported in the figure captions.

The error bars include counting statistics for the beam polarization and analyzing power data and statistical errors associated with the polarimeter analyzing powers [22]. Empirically determined correlations among the various sources of error have been taken into account in the error estimates. In addition to the statistical errors shown in the figures, an overall normalization uncertainty of 4% is present. This arises from using the quench-ratio method as the absolute polarization standard [12].

Our $^2H(d,p)^3H$ data are quite consistent with those measured at 30, 50, 70, and 90 keV by Tagishi *et al.* [12]. The $^2H(d,n)^3He$ reaction was not measured in Ref. [12]. This agreement is not surprising at forward angles since the data of [12] at 10 ° were used to calibrate our polarimeter, but it is heartening to note that the agreement extends throughout the angular range. As compared with the data of [11] at 28 keV, our data indicate somewhat larger values for the observables near 90 °. The results of [11] also indicate larger differences between the two reactions for $A_{xx} - A_{yy}$ than do our data at a reaction energy of 21 keV. Quantitatively, the ratio of the $A_{xx} - A_{yy}$ values at 90 ° for $^2H(d,n)^3He$ as compared to $^2H(d,p)^3H$ is about 0.76 for the data of [11], whereas this ratio is about unity for our data. Such a discrepancy for the two reactions cannot be attributed to an overall

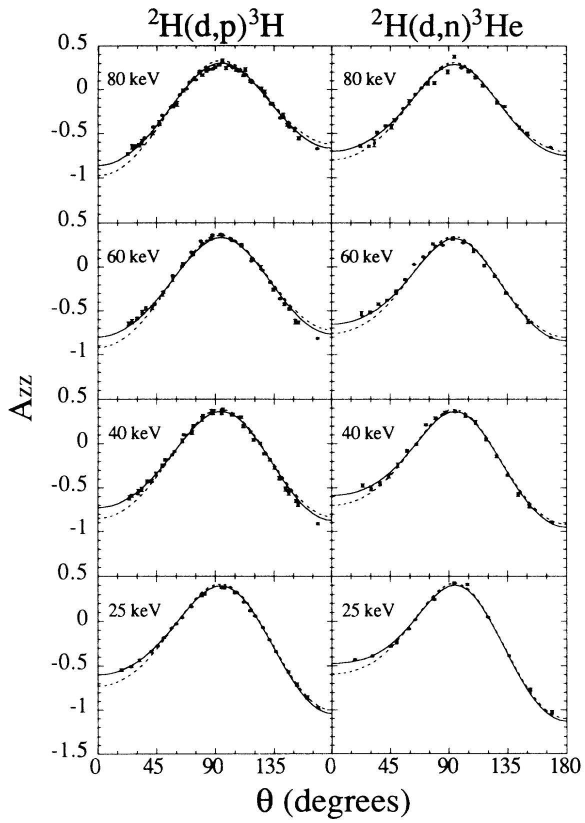

FIG. 2. Angular distributions of A_{zz} for the ^{2}H$(d,p)^3$H and ^{2}H$(d,n)^3$He reactions at laboratory bombarding energies of 25, 40, 60, and 80 keV. Because of energy averaging in the targets, the approximate reaction energies are 21, 39, 55, and 75 keV, respectively. The angles are measured in the c.m. frame. The error bars indicate statistical errors only, and the overall normalization error is 4%. The *dashed* lines indicate the R-matrix predictions made *before* our data were included in the data set. The *solid* lines indicate the R-matrix calculations for this observable *after* our data are included in the parametrization.

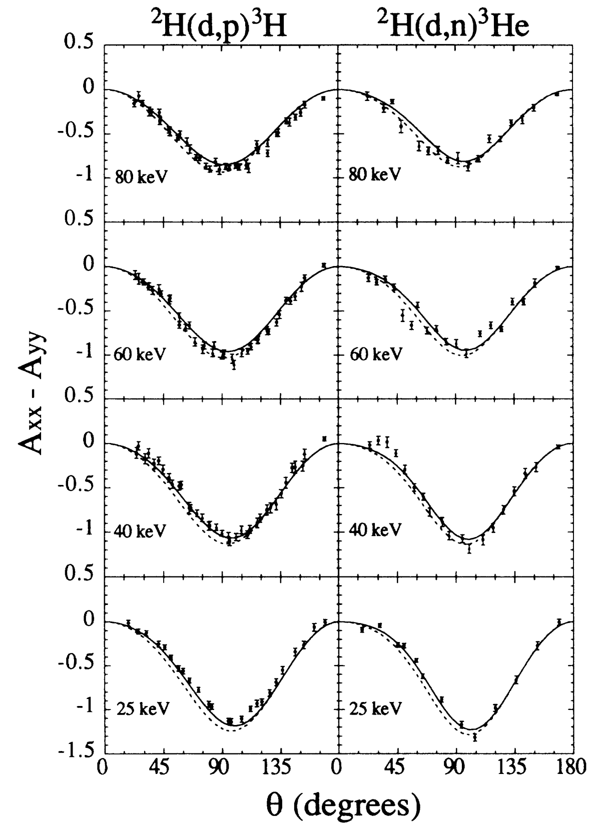

FIG. 3. Same as in Fig. 2 for the observable $A_{xx} - A_{yy}$. Because of differences in target thicknesses, the bombarding energies 25, 40, 60, and 80 keV correspond to reaction energies of 21, 38, 56, and 76 keV for this observable.

normalization error.

To directly compare the results for the two reactions, the data were fitted using a Legendre polynomial expansion, and the resulting curves are plotted in Fig. 4. In general, the analyzing powers for the two reactions are remarkably similar, with the largest deviations at forward angles for A_{zz}. As the energy increases, the values for A_{zz} at forward angles become slightly more negative, while those at backward angles become less so. Values of $A_{xx} - A_{yy}$ near 90° become less negative with increasing energy.

DISCUSSION

An R-matrix parametrization which *did not* include our low-energy tensor analyzing powers was used to predict the values of A_{zz} and $A_{xx} - A_{yy}$ at our reaction energies. The *dashed* lines in Figs. 2 and 3 show these predictions, which represent the data remarkably well, except at the most forward and most backward angles. The R-matrix calculations which *include* our data in the fit are represented by the *solid* lines. The discrepancies at the extreme angles are corrected when our data are included in the fit, as expected.

It has been shown [29] that the ratio of the neutron to proton yields obtained at room temperature in muon-catalyzed fusion of the ^{2}H+^{2}H reactions is equal to the ratio of the P-wave cross sections for ^{2}H$(d,n)^3$He to ^{2}H$(d,p)^3$H at low energies. This P-wave branching ratio, as determined from the present R-matrix analysis at 25 keV, is 1.39, which agrees with the value of 1.39±0.04 from muon-catalysis experiments [30].

The entrance quintet-S states γ_1 and δ_1 (using the notation of [8], and [6]), which have been ignored in earlier analyses [1,16], are, in fact, of the same order of magnitude as the singlet-S to singlet-S transition α_0. The ratios γ_1/α_0, and δ_1/α_0, calculated from the R matrix with our data included in the parametrization, are shown in Table I. From this table it is evident that quintet-S states are of considerable importance in these reactions. Similar ratios were reported for ^{2}H$(d,n)^3$He in [8] as 0.34 and 0.43, respectively. However, these are ratios of "energy-independent" internal matrix elements using a model as-

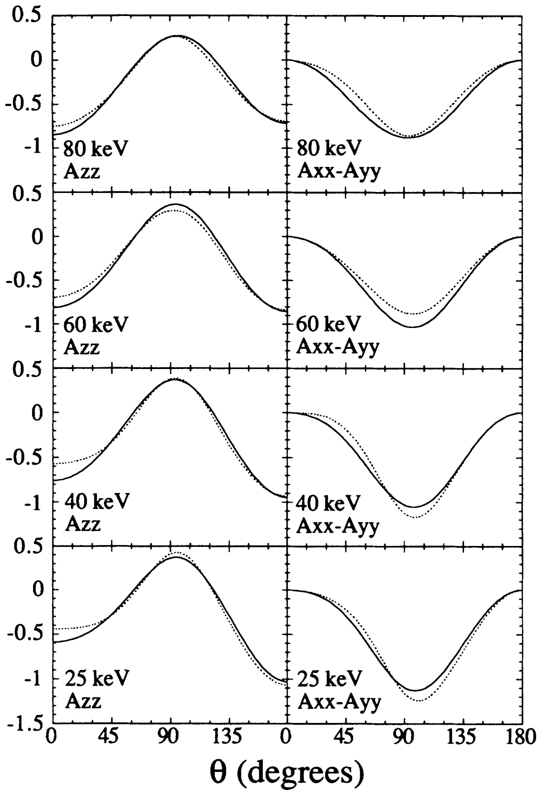

FIG. 4. Comparisons of Legendre function fits to the A_{zz} and $A_{xx} - A_{yy}$ data for ^{2}H$(d,p)^3$H (solid lines) and ^{2}H$(d,n)^3$He (dotted lines).

sumption that the energy dependence of the matrix elements is due to Coulomb and centrifugal barriers in the entrance channel. As discussed in [3], the quintet-S transitions near the ^{2}H+^{2}H threshold (which corresponds to an excitation energy of 23.85 MeV in ^{4}He) results from the very broad ($\Gamma_d = 8.21$ MeV) quintet-S level in ^{4}He at 27.42 MeV, and hence the appropriate matrix elements have an energy dependence determined by the resonance properties.

TABLE I. Matrix element ratios γ_1/α_0 and δ_1/α_0.

$E_d = 25$ keV	γ_1/α_0	δ_1/α_0
^{2}H$(d,p)^3$H	0.97	1.44
^{2}H$(d,n)^3$He	1.07	1.29
E_d=80 keV		
^{2}H$(d,p)^3$H	1.03	1.53
^{2}H$(d,n)^3$He	1.13	1.37

R-matrix parametrization which includes our data was used to calculate the polarized cross sections as a function of energy. In Table II these are expressed as ratios of the cross section for both deuterons polarized, integrated over all incoming directions [32],

$$\bar{\sigma}_{m,n} = \frac{1}{4\pi} \int d\Omega_{k'} \int d\Omega_k \sigma_{m,n}(\mathbf{k}', \mathbf{k}), \tag{2}$$

to that for unpolarized reactants σ_0. In the above expression, $\sigma_{m,n}(\mathbf{k}', \mathbf{k})$ is the center-of-mass differential cross section for deuterons having spin projections m and n on the quantization axis colliding with relative momentum $\mathbf{k}$ to form reaction products with relative momentum $\mathbf{k}'$, the magnitudes of $\mathbf{k}$ and $\mathbf{k}'$ being related by energy conservation. Our data are consistent with previous conclusions, first reported in [31] and [32] and more recently in [14,8,11,33] that polarizing the nuclei spin parallel in a fusion reactor will not strongly suppress the neutron or triton yield from the ^{2}H+^{2}H reactions.

TABLE II. Results of the R-matrix analysis: Polarized ^{2}H+^{2}H reaction cross sections averaged over incident directions.[a]

E_d (keV)	σ_0 (mb)	$\frac{\bar{\sigma}_{1,1}}{\sigma_0}$	$\frac{\bar{\sigma}_{1,0}}{\sigma_0}$	$\frac{\bar{\sigma}_{1,-1}}{\sigma_0}$	$\frac{\bar{\sigma}_{0,0}}{\sigma_0}$
		^{2}H$(d,p)^3$He			
10	9.019×10^{-3}	1.414	0.948	0.638	1.105
50	4.516	1.278	1.006	0.716	0.988
100	15.343	1.135	1.065	0.800	0.870
150	25.006	1.021	1.111	0.868	0.779
200	32.944	0.931	1.145	0.924	0.709
300	45.061	0.800	1.192	1.008	0.616
400	53.862	0.713	1.219	1.068	0.561
500	60.483	0.652	1.234	1.114	0.531
		^{2}H$(d,n)^3$He			
10	8.852×10^{-3}	1.295	0.989	0.717	1.023
50	4.620	1.123	1.061	0.815	0.877
100	16.345	0.960	1.129	0.911	0.741
150	27.466	0.838	1.178	0.983	0.643
200	37.028	0.748	1.214	1.039	0.572
300	52.244	0.624	1.260	1.116	0.480
400	63.621	0.547	1.286	1.167	0.428
500	72.251	0.496	1.301	1.204	0.399

[a]The average polarized cross secton satisfy $(2\bar{\sigma}_{1,1} + 4\bar{\sigma}_{1,0} + 2\sigma_{1,-1} + \sigma_{0,0})/9 = \sigma_0$.

SUMMARY

Angular distributions of the tensor analyzing powers A_{zz} and $A_{xx} - A_{yy}$ for the reactions $^2H(d,p)^3H$ and $^2H(d,n)^3He$ have been measured at incident deuteron energies of 25, 40, 60, and 80 keV. At each energy the observables differ only slightly for the two charge-symmetric reactions. The $^2H(d,p)^3H$ data are quite consistent with the recent 30-, 50-, 70-, and 90-keV data of [12].

These data have been included in a global R-matrix analysis of the four-nucleon system. From this analysis, the P-wave branching ratio was found to agree with the empirical value determined from muon-catalyzed fusion experiments. The ratios of quintet-S state to singlet-S state transitions were found to be of order unity, indicating that entrance-channel quintet-S state transitions should not be ignored in any analysis of these reactions. This indicates, contrary to earlier suggestions [15], that polarizing the fusion plasma in a $^3H(d,p)^4He$ reactor would not suppress the yield of the neutron-producing $^2H(d,n)^3He$ reaction.

ACKNOWLEDGMENTS

This work was supported by the U.S. Department of Energy through Grant No. DE-FG05-88ER40442. The authors wish to thank Dr. Y. Tagishi of the University of Tsukuba, Japan, Dr. G. Clausnitzer of Universität Giessen for providing assistance in target fabrication, and W. J. Thompson for advice on the reduction of the data. In addition, we thank T. B. Clegg, E. R. Crosson, S. K. Lemieux, J. C. Blackmon, B. Kozlowska, and L. Ma for their help in the collection of the data.

[1] E. J. Konopinsi and E. Teller, Phys. Rev. **73**, 822 (1948).
[2] H. Paetz gen. Schieck, Few-Body Syst. **5**, 171 (1988).
[3] D. R. Tilley, H. R. Weller, and G. M. Hale, Nucl. Phys. **A541**, 1 (1992).
[4] R. E. Brown and N. Jarmie, Phys. Rev. C **41**, 1391 (1990).
[5] A. Kraus, H. W. Becker, H. P. Trautvetter, C. Rolfs, and K. Brand, Nucl. Phys. **A465**, 150 (1987).
[6] B. P. Ad'yasevich and D. E. Fomenko, Yad. Fiz. **9**, 283 (1969) [Sov. J. Nucl. Phys. **9**, 167 (1969)].
[7] B. P. Ad'yasevich, V. G. Antonenko, and D. E. Fomenko, Yad. Fiz. **33**, 601 (1981) [Sov. J. Nucl. Phys. **33**, 313 (1981)].
[8] S. Lemaître and H. Paetz gen. Schieck, Few-Body Syst. **9**, 155 (1990).
[9] E. Pfaff, A. Hofmann, E. Huttel, N. Kniest, M. Nau, G. Reiter, S. Tharraketta, and G. Clausnitzer, J. Phys. Soc. Jpn. Suppl. **55**, 894 (1986).
[10] E. Pfaff (private communication).
[11] B. Becker, R. Randermann, B. Polke, S. Lemaître, R. Reckenfelderbäumer, P. Niessen, G. Rauprich, L. Sydow, and H. Paetz gen. Schieck, Few-Body Syst. **13**, 19 (1992).
[12] T. Tagishi, N. Nakamoto, K. Katoh, J. Togawa, T. Hisamune, and T. Yoshida, Phys. Rev. C **46**, R1155 (1992).
[13] G. M. Hale, Muon Catalyzed Fusion **5/6**, 227 (1990/91).
[14] H. M. Hofmann, G. M. Hale, and R. Wölker, in *Proceedings of the International Workshop on Few-Body Approaches to Nuclear Reactions in Tandem and Cyclotron Energy Regions,* edited by S. Oryu and T. Sawada (World Scientific, Singapore, 1987).
[15] K. M. Kulsrud, H. P. Furth, M. J. Valeo, and M. Goldhaber, Phys. Rev. Lett. **49**, 1248 (1982).
[16] J. R. Rook and L. J. Goldfarb, Nucl. Phys. **27**, 79 (1961).
[17] E. R. Crosson, K. A. Sweeton, H. Pfutzner, W. S. Wilburn, A. W. Lovette, T. B. Clegg, and H. J. Karwowski, Nucl. Instrum. Methods (to be submitted).
[18] T. B. Clegg, W. M. Hooke, E. R. Crosson, A. W. Lovette, H. Middleton, H. Pfutzner, and K. A. Sweeton, Nucl. Instrum. Methods (to be submitted).
[19] D. Dinge, T. B. Clegg, E. R. Crosson, and H. W. Lewis, Nucl. Instrum. Methods (to be submitted).
[20] H. H. Anderson and J. F. Ziegler, *Hydrogen Stopping Powers and Ranges in All Elements* (Pergamon Press, New York, 1977).
[21] Y. Irie, H. Yamamoto, H. Hasuyama, and Y. Wakuta, Genshikaku-Kekyu **17**, 567 (1973).
[22] K. A. Fletcher, T. C. Black, H. J. Karwowski, E. J. Ludwig, and Y. Tagishi, Nucl. Instrum. Methods A **329**, 197 (1992).
[23] *Proceedings of the Third International Symposium on Polarization Phenomena in Nuclear Reactions*, Madison, Wisconsin, 1970, edited by H. H. Barschall and W. Haeberli (University of Wisconsin Press, Madison, 1971), p. xxv.
[24] P. L. Kapur and R. Peierls, Proc. Soc. London A **166**, 277 (1938).
[25] E. P. Wigner and L. Eisenbud, Phys. Rev. **72**, 29 (1947).
[26] A. M. Lane and R. G. Thomas, Rev. Mod. Phys. **30**, 257 (1958).
[27] G. M. Hale and D. C. Dodder, in *Proceedings of the International Conference on Nuclear Cross Sections for Technology*, Knoxville, 1979, edited by J. L. Fowler, C. H. Johnson, and C. D. Bowman, Natl. Bur. Stand. (U.S.) Spec. Publ. No. 594 (U.S. GPO, Washington, D.C., 1980), p. 650.
[28] G. M. Hale, D. C. Dodder, J. D. Seagrave, B. L. Berman, and T. W. Phillips, Phys. Rev. C **42**, 438 (1990).
[29] L. N. Bogdanova, V. E. Markushin, V. S. Melezhik, and L. I. Ponomarev, Phys. Lett. **115B**, 171 (1982).
[30] D. V. Balin, E. M. Maev, V. I. Medvedev, G. G. Semenchuk, Yu. V. Smirenin, A. A. Vorobyov, An. A. Vorobyov, and Yu. K. Zalite, Phys. Lett. **141B**, 173 (1984).
[31] G. M. Hale, in Proceedings of the Polarized-Fuel Reactor Workshop, Madison, WI, 1983 (unpublished).
[32] G. M. Hale and G. D. Doolen, Los Alamos Report No. LA-9971-M5, 1984.
[33] H. Paetz gen. Schieck, B. Becker, R. Randermann, S. Lemaître, P. Niessen, R. Reckenfelderbäumer, and L. Sydow, Phys. Lett. B **276**, 290 (1992).